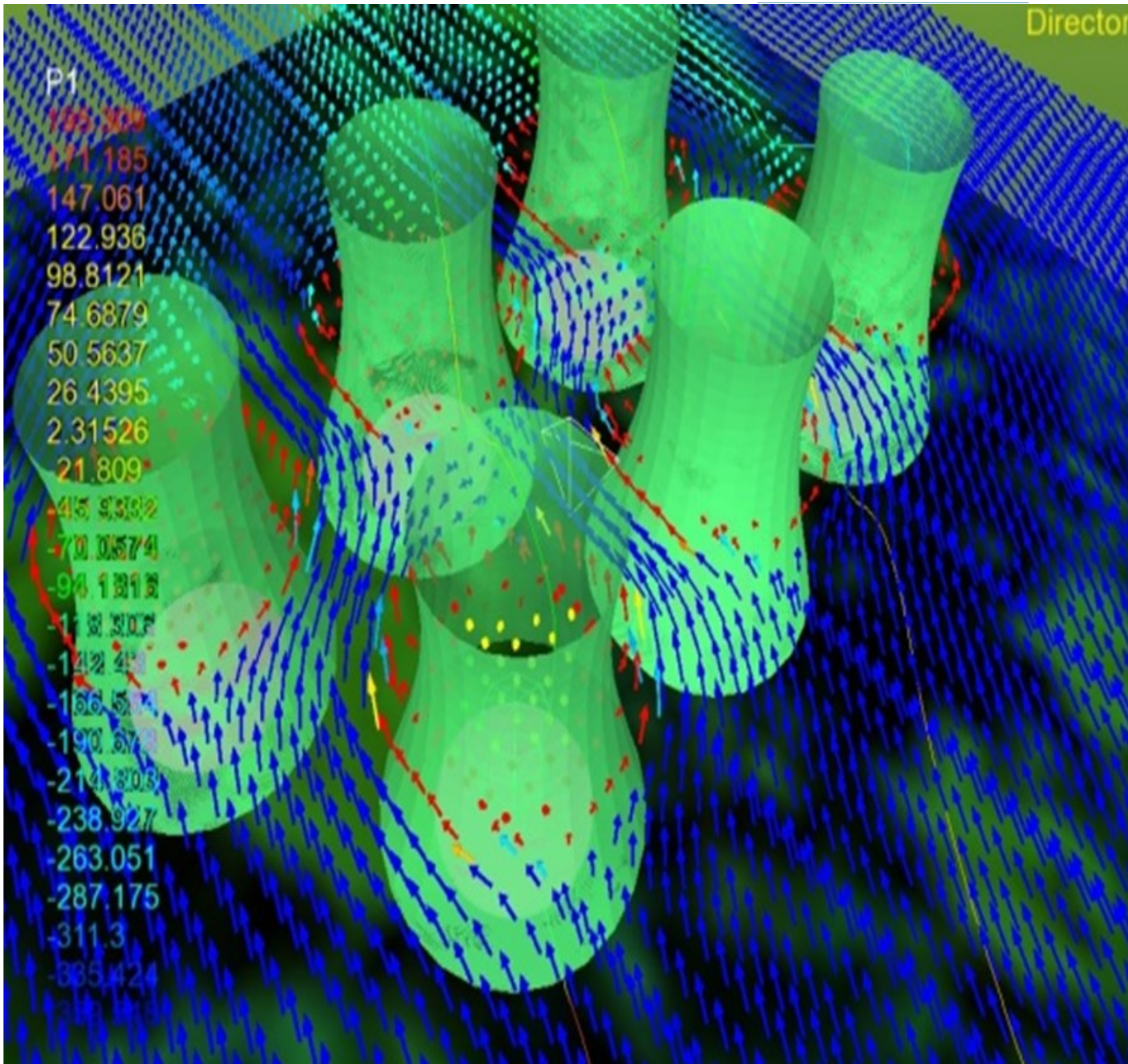


PHOENICS NEWS



PHOENICS – Empowering Engineers

Winter 2015



P1
195.809
171.185
147.061
122.936
98.8121
74.6879
50.5637
26.4395
2.31526
21.809
-45.9332
-70.0574
-94.1816
-118.305
-142.429
-166.553
-190.677
-214.801
-238.927
-263.051
-287.175
-311.3
-335.424

Director

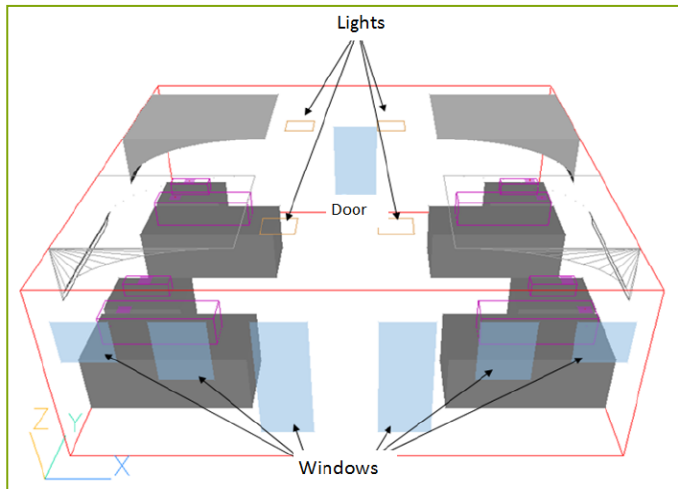


Figure 1 - Base-Case. M1, B1 (Bottom left), M2, B2 (Top Left), M3, B3 (Bottom Right) and M4, B4 (Top Right).

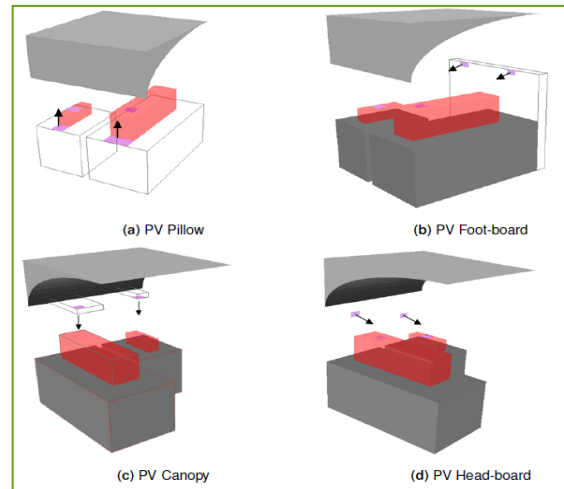


Figure 2 - PV Configurations

Performance of personal ventilation systems in a multi-bed maternity ward

Thomas Corbett, Malcolm J. Cook, Dennis L. Loveday.

School of Civil and Building Engineering, Loughborough University, Leicestershire, LE11 3TU, UK.

Personal ventilation is a method of supplying a small zone within a space with cool fresh supply air for the purpose of improving the quality of air inhaled by the occupants. Many studies have demonstrated positive benefits of personal ventilation in office environments, but little is reported for hospitals. The lower energy consumption and improved control associated with personal ventilation systems could not only improve indoor air quality for hospital patients but could also reduce the hospital's energy use and running costs.

The main aim of the study reported here was to explore the effects of providing different ventilation rates using different designs of personal ventilation systems. PHOENICS was used to evaluate the potential of four different personal ventilation configurations for delivery of air to patients whilst in their beds: canopy, pillow, headboard and footboard-based systems.

A typical four-bed maternity ward ($8 \times 8 \times 3$ m) comprising four mothers (M1-M4) and four babies (B1-B4) was modelled (Figure 1), with a total openable window area of 3.83m^2 on the opposite side to the door opening, to provide the background (natural) portion of the ventilation requirements. A base case simulation was used in which natural ventilation from 6 openings on a single side of the ward was modelled. Each ventilation scenario was modelled with and without an open door on the opposite side (Figure 1).

The four ventilation systems examined could readily be installed into hospital bed designs or into the hospital ward itself. As humans are sensitive to variations in temperature and air movement, providing uniform conditions across the body was considered a desired outcome.

Occupant breathing was modelled using inhalation rates of $1.5 \times 10^{-4} \text{m}^3/\text{s}$ (for the mothers) and $2.5 \times 10^{-5} \text{m}^3/\text{s}$ (for the babies). Each personal ventilation strategy was modelled using supply rates of 0.3, 5 and 8 litres per second per person. PHOENICS was used to determine the quality of the air to which the mothers and their babies would be exposed for each configuration. The mean age of air, air temperature and air velocities were predicted throughout the domain.

We, at CHAM, would like to wish our Agents, and PHOENICS Users worldwide, a Merry Christmas and a Happy New Year.

We look forward to working with you in 2016.

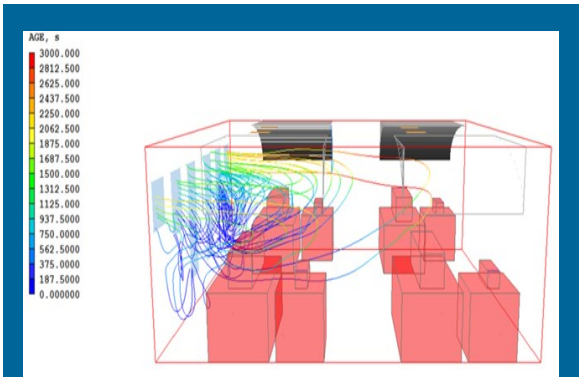
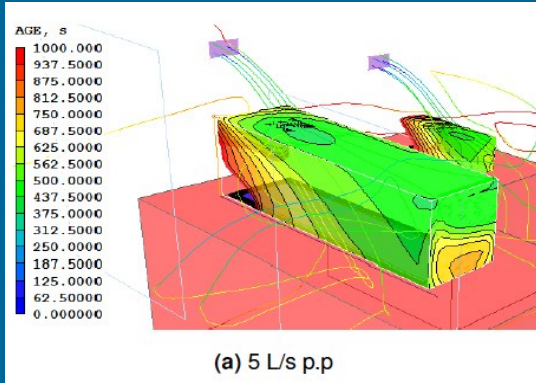
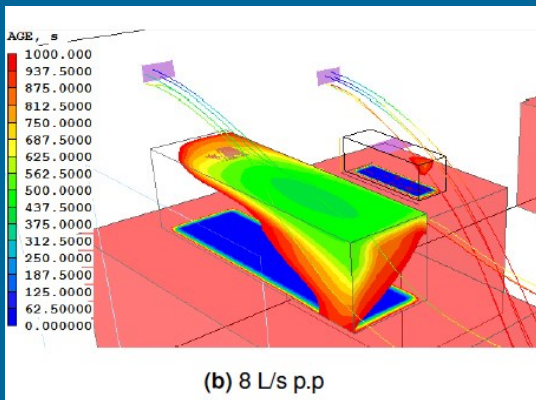


Figure 3—Single-sided base cse scenario



(a) 5 L/s p.p



(b) 8 L/s p.p

Figure 4—Age of air (s) contours for different ventilation rates delivered by the PD headboard system, ,

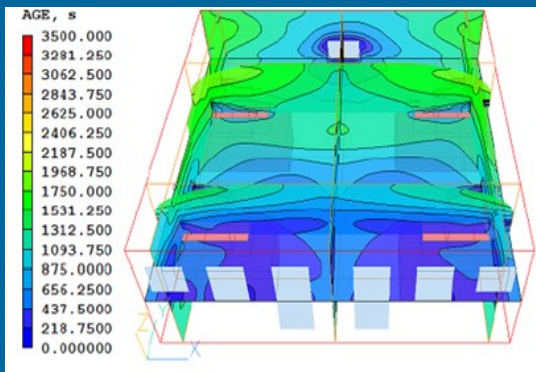


Figure 5—Age of air (s) contours for PV headboard using 8 litres per second per person.

Figure 3 shows streamlines initiated at the windows coloured by the age of air. This provides a useful insight into how the freshest air flows at low level across the patients, before warming and leaving the space. The results clearly show that air does not penetrate deep into the space, resulting in a lack of fresh air in some zones, and leading to the creation of stale air zones.

Using streamlines and surface contours, it was possible to see the age of air across the surface of mothers and babies, as well as the age of air within their breathing zone, thus providing a prediction of the quality of inhaled air. Figure 4 demonstrates the short-circuiting effect resulting from using an increased ventilation rate. It shows that when 8 litres per second was used (Figure 4b), a large proportion of air travelled directly over mothers and their babies before sinking, whereas figure 4a shows how a smaller ventilation rate would expose the patient to younger, therefore fresher, air.

It can be seen from figure 5 that the youngest air for the headboard case accumulates at low level near to openings. The young air surrounding the door on the back wall in figure 5 shows some evidence of a bi-directional flow. Nevertheless, it can be seen that there is variation in age of air between patients, with those near to the door being exposed to air almost twice the age of that near to the openings. The nominal time constant of a ventilated space is the ratio of its volume to the volumetric supply flow rate of fresh air, which has been shown to equate to the mean age of air at the exhaust. This was used to give an indication of the quality of air and distribution of fresh air. The nominal time constant was later used to calculate the local air change effectiveness of the system.

Local air change effectiveness describes the system's ability to supply air into a certain zone; it is the ratio of nominal time constant and mean age of air within a zone, in this case breathing zones of mothers and babies. For the example in figure 5, the nominal time constant was 2119 seconds. Using this as a guide, it can be seen that almost the entire space contains air with an age which is less than this value. This means the air inhaled by mothers and babies is half the age of that being exhausted from the space. A local air change effectiveness of unity indicates that the air distribution system delivers air equivalent to that of a perfectly mixed space.

The fact that figure 5 shows nearly all mothers and babies are exposed to a local air change effectiveness of greater than unity suggests this system's ability to deliver air to the intended zone is very good.

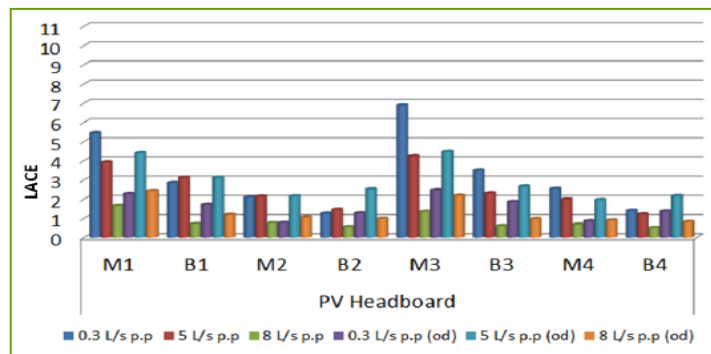


Figure 6 - Local Air Change Effectiveness (LACE) for all supply rates from the PV Headboard

All patients have been modelled with their breathing zone facing the ceiling (i.e. lying in bed on their backs). Nevertheless, a hospital environment is arguably the only mechanically ventilated one where it would be expected that the occupants' breathing zones would also face to the left or right, for example through involuntary movement during sleep. This is an important characteristic of hospital ventilation design that needs to be considered for bed-centred localised/personal ventilation system.

Patient movement during the day and night was therefore emulated by modelling the breathing zone on both sides of the patient's head in separate simulations. Comparing the air velocity, age and temperature within the breathing zone of patients, for both breathing locations, allowed the effect of this movement on the effectiveness of the system to be determined. Predictions for the head and foot –board systems indicated a similar quality of air in the breathing zone (Figure 7). Averaging the age of air inhaled by all patients for each ventilation scenario made for an easier comparison and removed any positioning bias created by the difference in distance from the window openings among all patients .

Analysis of surface 'age of air' contours taken from the bodily surface of the mothers and babies, allowed the variation in air velocity and temperature across the patients' bodies to be examined. The canopy system supplied the breathing zone with the youngest air of all the systems tested. However, this system created a significant variation in thermal and air speed across the body. The uncovered head was exposed to cool fast moving air, potentially posing a draught risk. The predictions of temperature variation across the body of the mothers are shown in figure 8. The large decrease in temperature surrounding the head region when using the PV canopy system demonstrates the potentially uncomfortable flow of high velocity supply air .

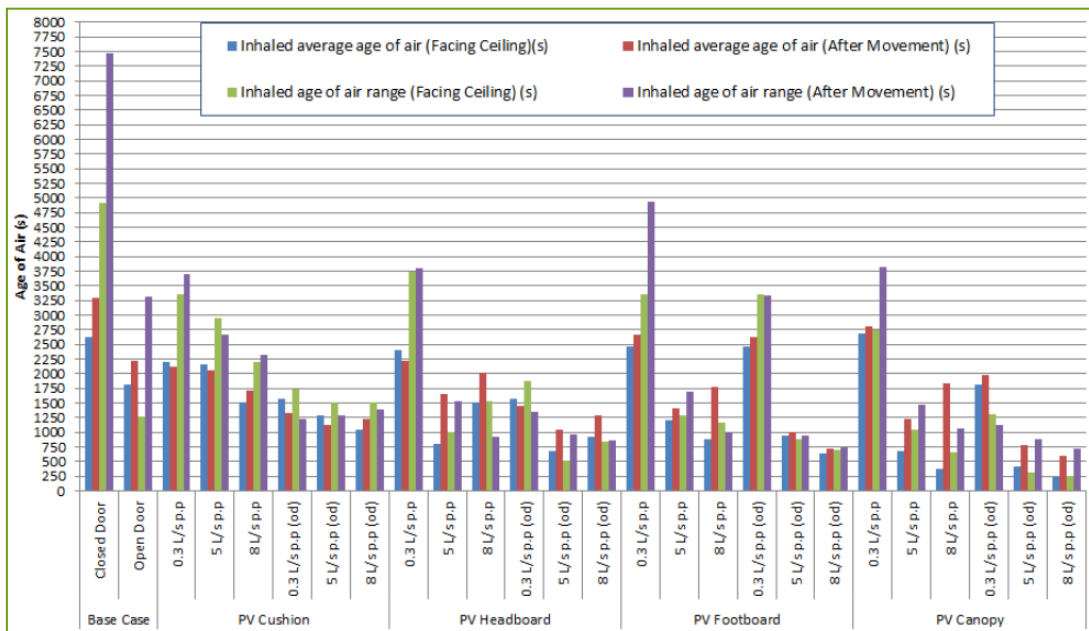


Figure 7 - Average and range of inhaled air age across all patients for all PV configurations and base-case scenarios. (After movement represents the patients rolling onto their sides.)

Figure 8 below also highlights the 'short-circuiting' phenomena, which is associated with the horizontal delivery of high velocity supply air. Focusing on the headboard system, the simulations show that increasing the supply rate results in cooling being provided lower down the body. As a result of this, supply air intended for the breathing zone has travelled above this region, leaving it unconditioned and thus providing no benefit to the patient, potentially leading to discomfort.

The study showed that to accommodate patient movement, a small compromise in air quality was required in order to provide the desired uniform conditions and avoid draughts. The PHOENICS simulation work has shown a range of capabilities offered by each of the four configurations investigated, and experimental validation is currently underway. It is expected that the work will help support recommendations to aid selection of suitable bed-centred personal ventilation systems for hospital ward application, incorporating energy performance as one of the evaluation criteria

News from ACFDA (Canada)

1) A PHOENICS CFD model of supercritical fluid flow and heat transfer was presented at the 16th Int. Topical Meeting on Nuclear Reactor Thermal Hydraulics (NURETH-16) in Chicago, USA (Sep 4, 2015). Details in http://www.acfda.org/results/NURETH-16_Final_Paper_13732rev8.pdf.

2) A novel physics-based multi-phase CFD model of wildland fire initiation and spread, WILDFIRE, has been implemented in PHOENICS and validated for surface wildfires. The model will be presented at the 5th Int. Fire Behavior & Fuels Conference, Portland, Oregon, USA in April 2016. It accounts for drying, pyrolysis, char combustion, turbulent gaseous combustion, interphase exchange of mass, momentum and energy and radiative heat transfer. A brief description is in http://www.acfda.org/results/Abstract_Agraat_Perminov_Portland_2016.pdf; Details from vlad@acfda.org.

3) Standard and customized PHOENICS CFD software training courses are arranged by ACFDA in Toronto, on client sites and over the internet. Advanced topics include multi-phase modeling options, combustion models, CFD applications to risk/safety analyses and specific client applications. Among customized CFD models offered are GFLOW (complex gas-liquid flows), GRAD (flammable/toxic gas release/dispersion), TPLUME (two-phase plumes from industrial installations), SCFLOW (supercritical fluid flow and heat transfer), WILDFIRE (wildland fire initiation and spread). Details: info@acfda.org.

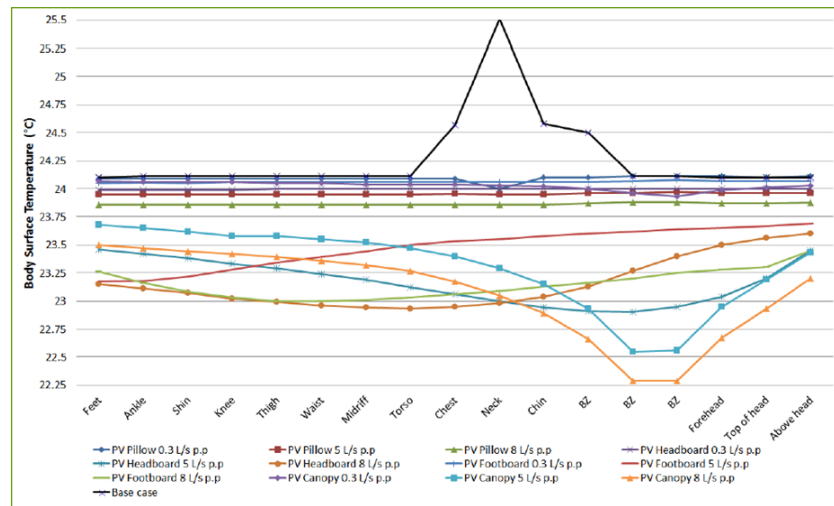


Figure 8—Body surface temperature variation across mother 1.

Solid Particle Flow in a Full-Scale Blast Furnace

Reza Safavi Nick, Swerea MEFOS, Lulea, Sweden

1) Introduction

A blast furnace reactor is probably one of the most complex operating systems in process metallurgy. Modern blast furnaces might operate with up to four phases, i.e. gas, solid particles, fine powder and liquid. Pig-iron is produced in a blast-furnace, and the raw materials needed for its production are iron ore and coke. Of course, there are other methods of producing pig iron, such as for example Direct Reduction Iron (DRI), but the scale and level of production rate realised in a blast furnace probably makes it the most effective iron-making process known today. Nevertheless, there is a need to improve blast-furnace practice because of the increasing demand for clean industry and a reduction of greenhouse gases.

In a blast furnace, such as the SSAB Oxelösund (Fig 1), the solid particles, e.g. iron pellets, coke, are fed from the top of the furnace, while the hot blast is injected through the tuyeres located at the lower part of the furnace. Of course, the solid particles travel slowly downwards, while the hot blast ascends through layers of packed material. The high temperature blast generates a chain of reactions in which the raw materials, pellets, will transform into the liquid state.

The iron-making blast furnace is essentially a counter-flow, multiphase, chemical reactor, where each of the existing phases can be assumed to behave like interpenetrating continua. Consequently, the blast-furnace system can be modelled as multi-phase fluid flow in an Eulerian frame of reference with suitable closure models for the various momentum, heat and mass transfer processes.

The overall objective is to develop a PHOENICS-based CFD model of a blast furnace for computing the various phase distributions within the system. The present article focuses on work performed so far to extend the two-phase, Eulerian-Eulerian, interphase slip algorithm (IPSA) of PHOENICS to include some important physical aspects of solids flow within the reactor. For this purpose, numerical studies are carried out using a simplified two-dimensional, two-fluid, cold-flow model of the gas and solid phases under conditions representative of a full-scale blast furnace.



Fig 1. SSAB Oxelösund blast furnace Sweden. Courtesy of Erik Olsson.

2. Modelling

The momentum equation for the solid phase can be written as follows: (1)

$$\frac{\partial(\rho_s \varepsilon_s \bar{u}_s)}{\partial t} + \nabla \cdot (\rho_s \varepsilon_s \bar{u}_s \bar{u}_s) = -\varepsilon_s \nabla p - \beta(\bar{u}_s - \bar{u}_g) + \nabla \cdot (\tau_{rd} + \tau_{ri}) + \rho_s \varepsilon_s \bar{g}$$

where ε_s is the solid volume fraction, ρ_s is the solid density, \mathbf{u}_s and \mathbf{u}_g are the solid and gas velocity vectors, β is the interphase momentum transfer coefficient, \mathbf{g} is the gravitational vector, τ_{rd} is the rate-dependent part of surface stress tensor and

τ_{ri} is the rate-independent part. The variable τ_{rd} , originates from the particle-particle kinetic interaction due to collision, whereas τ_{ri} originates from particle-particle-contact interaction due to packing, including normal contact and shear friction. The rate-dependent part is the Newtonian part of the constitutive equation for the solid phase which can be written as:

$$\tau_{rd} = 2\varepsilon_s \mu_s D_s + \left(\lambda_s - \frac{2}{3}\mu_s\right) \varepsilon_s \text{tr} D_s I \quad (2)$$

where μ_s is the solids shear viscosity, and D_s is the deformation tensor:

$$D_s = \frac{1}{2}(\nabla \bar{u}_s + (\nabla \bar{u}_s)^T) \quad (3)$$

For simplicity, the bulk viscosity $\lambda_s = 0$, and the following formula is used for the solids viscosity [1]:

$$\mu_s = 0.0165 g_o \varepsilon_s^{1/3} \quad (4)$$

where the radial distribution function, g_o , is given by:

$$g_o = \left[1 - \left(\frac{\varepsilon_s}{\varepsilon_{s,m}} \right)^{1/3} \right]^{-1} \quad (5)$$

where in the present study, $\varepsilon_{s,m} = 0.67$. The radial distribution function is a correction factor that modifies the probability of collision close to packing.

The rate-independent part is based on the Coulomb frictional relation and can be expressed as follows:

$$\tau_{ri} = -P_e I + 2\eta_s \frac{D_s}{\sqrt{\text{tr} D_s^2}} \quad (6)$$

where P_e is the effective solids pressure and η_s is the coefficient of plastic modulus. The variable η_s can be determined as follows [2]: (7)

$$\eta_s = \frac{1}{\sqrt{2}} (\alpha_1 + \alpha_2 P_e^n)$$

where α_1 is equal to zero for cohesionless materials and $n=1$ corresponding to the Coulomb frictional model. In addition, the friction coefficient α_2 can be expressed as follows:

$$\alpha_2 = \frac{\left| \frac{\partial w_s}{\partial x} \frac{1}{w_s} \right|}{\left| \frac{\partial w_s}{\partial x} \frac{1}{w_s} \right|_{Max}} \tan \phi \quad (8)$$

where ϕ is the internal friction angle, and Max denotes the maximum value in the flow field.

The solids pressure P_e is modelled by using the following constitutive equation [3,4]:

$$P_e = \frac{G_0}{c} e^{c(\epsilon_s - \epsilon_{s,m})} \quad (9)$$

where G_0 is the reference elastic modulus, c is the compaction modulus, and $\epsilon_{s,m}$ is the packing density or solid volume fraction measured under the standard loose or poured packing condition.

3. Implementation of the solids-pressure term

If equation (6) is substituted into the momentum equation (1), an additional pressure gradient appears for the solids pressure term, which can be written as:

$$-\nabla P_e = -\frac{\partial P_e}{\partial \epsilon_s} \nabla \epsilon_s = -G_s \nabla \epsilon_s \quad (10)$$

where G_s is the elastic modulus, which is defined by

$$G_s = G_0 e^{c(\epsilon_s - \epsilon_{s,m})} \quad (11)$$

The solids pressure represents the normal forces due to particle-particle interactions, and it prevents the solids phase from reaching unrealistically high volume fractions, which also promotes numerical stability. The following values have been used for the empirical constants: $G_0=1.0\text{Pa}$, $c=150.0$ and $\epsilon_{s,m}=0.62$.

The discretised form of the solids-pressure force in direction i is

$$F_i = G_s A_i (\epsilon_{s,i} - \epsilon_{s,i+1}) \quad (12)$$

where A_i is the flow area in the direction i . Implementation of the solids-pressure term involves three area-type PATCHES that introduce a solids-pressure force explicitly in each coordinate direction, as defined by PIL and INFORM command.

4. Implementation of the solids shear viscosity

For both phases, by default PHOENICS neglects any momentum source terms arising from the viscous stress tensor, which means that the effects of viscosity are represented solely through the diffusive transport terms. The solids shear viscosity m_s appearing in the diffusion terms of the solids momentum equation is computed from equation (4). It is implemented in PHOENICS through the Q1 file by using PIL and INFORM commands to calculate the kinematic viscosity used in each solids momentum equation:

5. Boundary and Initial Conditions

The foregoing extension to IPSA has been tested on a simplified 2D model of reduced furnace dimensions, and the simulation is advanced in time using a time of 5ms. The gas density is 1.189 kg/m^3 , the solids density is 3700 kg/m^3 , and inter-phase drag is modelled using the built-in particle-fluidisation model, which switches to the well-known Ergun equation for $\epsilon_s > 0.8$. It should be mentioned that the coefficient of plastic modulus h_s appearing in equation (6) above has been set to zero in these preliminary studies.

Initial conditions are stagnant flow with $\epsilon_s=0.71$. The boundary conditions are:

Top boundary Solid phase: - Fixed mass inflow rate with $\epsilon_s=0.01$.
 Gas phase: - Fixed pressure

Bottom boundary Solid phase - Fixed mass outflow rate equal to solids mass inflow rate
 Gas phase: - Fixed mass inflow rate with $\epsilon_s=0.71$.

The top boundary represents the stockline of the blast furnace, which is the top surface of the solid packed bed of material.

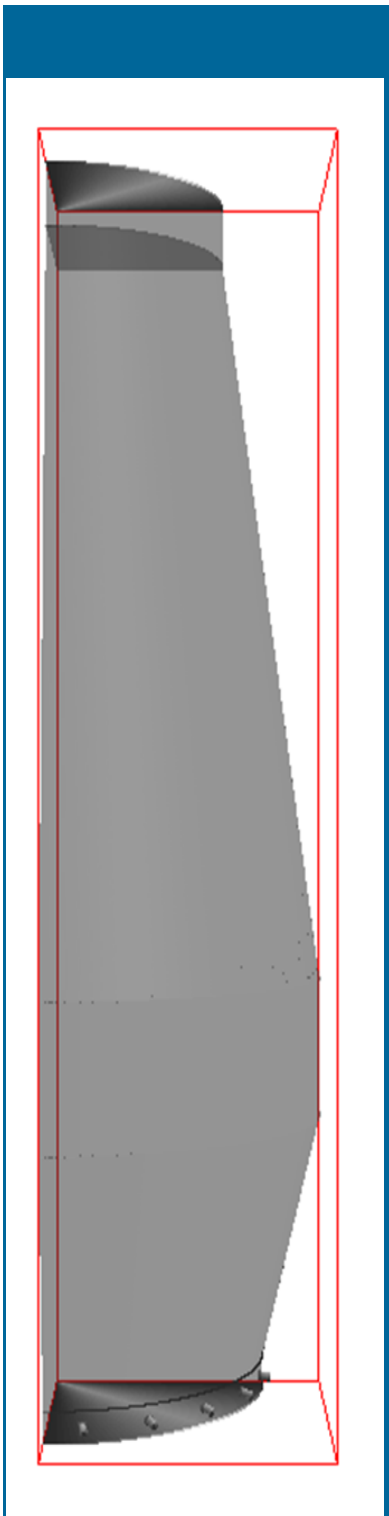


Fig. 4. A Real dimension blast furnace

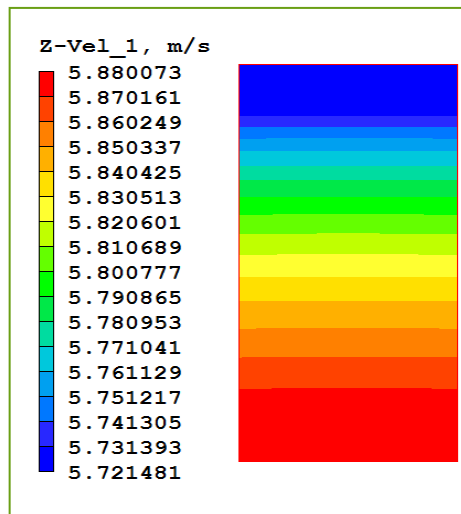


Fig 2.1 gas velocity profile for a simplified 2D model

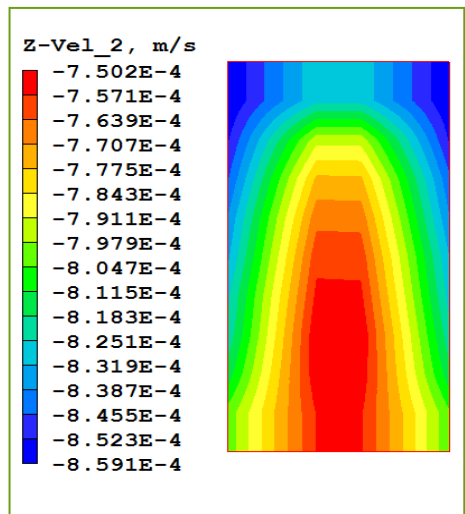


Fig 2.2 solid velocity profile for a simplified 2D model

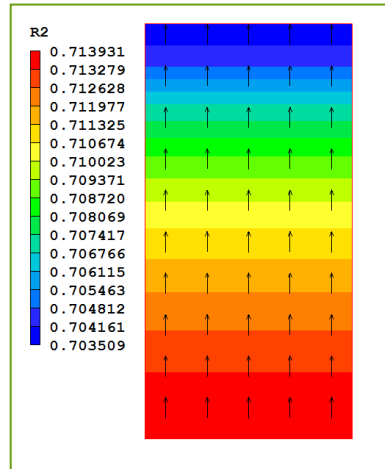


Fig 3.1 Vector field for the gas phase coloured by the solid phase volume fraction

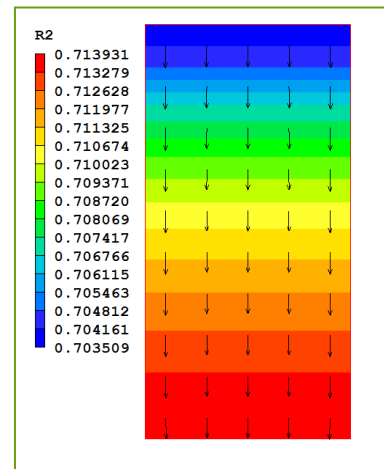


Fig 3.2 Vector field for the solid phase coloured by the solid phase volume fraction

6. Results and Future Work

Figs 2.1 and 2.2 present contour plots of the velocities for both phases, and Figs 3.1 and 3.2 show the vector vectors of the gas and solid phases, respectively, coloured by the solids volume fraction. It can be seen that model predicts the expected flow behaviour, namely the solid phase descends slowly through the furnace, while the gas phase ascends rapidly through the bed of solid material. The solid volume fraction at the bottom of the furnace (solid outlet) is greater than that at the top of the furnace (solid inlet). This is due to the weight of the bed above, which compresses the materials below. Furthermore, at the top of the domain (the solid inlet) solid particles are under significantly less stresses.

The next step will be to test the model by performing a simulation for flow through a full-scale blast furnace with the geometry shown in Fig 4 over the page.

7. References

- 1) H. Norem: Proc. the Davos Symposium, Avalanche Formation, Movements and Effects, IAHS, (1987).
- 2) S. J. Zhang, a. B. Yu, P. Zulli, B. Wright and U. Tüzün: ISIJ International, 38(1998), 1311.
- 3) C. Orr: Particulate Technology, Macmillan, New York, (1966)

PHOENICS Modelling of Indoor Aerosol Transport and Deposition

Bin Zhao+, Bin Zhou+ and Michael Malin*

+ Department of Building Science, School of Architecture, Tsinghua University, Beijing 100084, China, * Concentration Heat & Momentum Limited (CHAM)

The Department of Building Science at Tsinghua University has created a PHOENICS-FLAIR ground module for modelling the dispersion and deposition of aerosol particles in indoor environments. Typically, indoor particle sizes range from submicron to larger than 100 microns in diameter.

Aerosol particles are considered one of the main indoor pollutants; their modelling in enclosed spaces is important for studying indoor air quality and ventilation-systems design. Typical applications include human exposure to biological or radiological aerosols in healthcare or laboratory environments, health hazards from industrial aerosols in the work place and residential buildings, airflow pattern design in clean rooms (including protective environments and isolated rooms), and surface contamination by particle deposition on artworks, electronic equipment, etc.

CFD modelling of aerosols can use either a moving frame of reference (Lagrangian) or a fixed frame of reference (Eulerian), but the computational expense of the former has led to an extensive adoption of the Eulerian approach, which models each class of aerosol as a continuous phase, but at moderate computational cost. This type of aerosol transport model [1-4] presumes a very dilute two-phase flow with no collisions or coalescence, and drift-flux modelling is used to represent slippage between the particle and gas phases due to gravitational effects.

The origins of the drift-flux method can be traced back some fifty years [5], and its history in CFD modelling of multi-phase flows is almost as long [6]. It is only relatively recently that the method has been used for studying aerosol behaviour in enclosed building spaces [1-4].

The Eulerian aerosol model can be readily extended to include other slip mechanisms, such as for example thermophoresis and turbulence [4,7]. Coupling between the phases is one way, which means the particle concentration fields could be computed as a post-processing exercise by restarting from the converged hydrodynamics solution.

In the model, the surface deposition of particles is calculated by using semi-empirical wall models [8-12] which evaluate the local deposition rate as a function of particle size, density and friction velocity. These models can be extended to account for the re-suspension of deposited particles.

The PHOENICS implementation is restricted to cases using Cartesian meshes with slip in the gravitational direction, and optional deposition on horizontal and vertical surfaces without re-suspension. The default is no deposition with three alternative models for surface deposition, as follows: (a) gravitational settling on upward-facing horizontal surfaces; (b) deposition due to gravitational effects and Brownian diffusion using an analytical surface model [8-9]; and (c) deposition through the mechanisms of gravity, diffusion & turbophoresis [10-12]. These deposition models can be generalised to account for deposition on inclined surfaces within the framework of the Cartesian cut-cell solver, PARSOL.

The model has been exercised by Tsinghua University on a number of validation and application cases concerned with airborne particles in ventilation ducts and indoor room environments [7]. Further information on these simulations will appear in a future Newsletter.

References

- 1) S.Murakami, S.Kato, S.Nagano & Y.Tanaka, "Diffusion Characteristics of Airborne Particles with Gravitational Settling in a Convection-dominant Indoor Flow Field", ASHRAE Trans. 98: 82–97, (1992)
- 2) S.Holmberg, & Y.Li, "Modelling of the indoor environment—particle dispersion & deposition", Indoor Air, 8, 113–122, (1998)
- 3) F.Chen, C.M.Simon & A.C.K.Lai, "Modeling particle distribution and deposition in indoor environments with a new drift-flux model", Atmospheric Environment, 40, 2, 357-367, (2006).
- 4) B.Zhao, C.Chen & Z.Tan, "Modelling of ultrafine particle dispersion in indoor environments with an improved drift flux model", Aerosol Science 40, p29-43, (2009).
- 5) N.Zuber & J.A.Findlay, "Average Volumetric Concentration in Two-Phase Flow Systems", ASME J.Heat Transfer, 87,4, 453-468, (1965).
- 6) A.Artemov et al, "A tribute to D.B.Spalding and his contributions in science & engineering", Int J Heat & Mass Transfer, 52(9):3884-3905, (2009).
- 7) B.Zhao & B.Zhao, "Test of a generalised drift-flux model for simulating indoor particle dispersion", 7th Int. Symp Heating, Ventilation & Air Conditioning, II, 2: Indoor Environment, 382, (2011)
- 8) B.Zhao, X.Li & Z.Zhang, "Numerical study of particle deposition in two differently ventilated rooms", Indoor & Built Environment, 13, p443-451, (2004).
- 9) A.C.K.Lai & Nazaroff, "Modelling indoor particle deposition from turbulent flow onto smooth surfaces. Aerosol Sci. Technol. 31: 463–476, (2000).
- 10) B.Zhao & J.Wu, "Modelling particle deposition from fully developed duct flow", J. Atmospheric Environment, 40, p457-466, (2006).
- 11) V.N.Piskunov, "Parameterisation of aerosol dry deposition velocities onto smooth & rough surfaces", Aerosol Science 40 664-679, (2009).
- 12) R.You, B.Zhao & C.Chen, "Developing an empirical equation for modelling particle deposition velocity onto inclined surfaces in indoor environments", 46, p1090-1099, Aerosol Science & Technology (2012).

News from CHAM

Dr David Glynn gave a training course at Hyder Consulting, Hong Kong, in September 2015. The team principal, Gina Littlefair, is pictured with the rest of her design team.



News from CHAM Japan

PHOENICS was presented at an INCHEM Exhibition (November 25-27). Over 100 persons visited the stand to obtain information on the software. (<http://www.jma.or.jp/INCHEM/en>). Some 60 persons attended CHAM Japan's PHOENICS-2015 User Conference in Tokyo on October 9. **For Training Course and Seminar Dates visit www.phoenics.co.jp.**



Authors, and titles, of presentations are given below:
Introduction of the jet engine-related analysis case,
Manayuki Fujimoto, Aerospace Engine Group, Advanced Science & Intelligence Research Institute

Application of PHOENICS to the design to improve the stirring force in a constant temperature bath
Syouichiro Baba, Long-term Observation Technology Group, Ocean Engineering Center Marine Technology Development Department, Japan Agency for Marine-Earth Science & Technology

Comparison between Experimental Result & Numerical Analysis for Micromixing Flow Induced by Marangoni Convection on a Gas-Liquid Free Interface
T. Yamada & N. Ono, Mechanical Science & Engineering Department, Shibaura Institute of Technology

Encounters with the coagulation and melting calculation of PHOENICS
Masahiro Sugawara, Part-time lecturer, Akita University

Comparison of jet velocity distribution simulation and experimental results of wind tunnel
Prof. Syunichi Sakuragi, Mechanical Engineering Department, Shizuoka Institute of Science & Technology

Deployment of as an architectural design tool
Hironori Kimura, General Environmental Technology Office, Ishimoto Architectural & Engineering Inc.

Case Study of PHOENICS in the Company
Rina Kajita, Thermal Engineering & Development Co. Ltd.

Wake modelling: the actuator disc concept in PHOENICS

N. Simisioglou, (a)*, M. Karatsioris (b), S.P. Bretonb, S. Ivanell (b)
(a) WindSim AS, Fjordgaten 15, Tønsberg N-3125, Norway
(b) Wind Energy Section, Uppsala University Campus Gotland, Visby SE 621 67, Sweden

* Author to whom correspondence should be addressed, E-mail: nikolaos.simisioglou@windsim.com

Accurate modelling of wind turbine wakes is essential for the design and optimization of modern wind farms. The study presents a computational approach which extracts energy from the flow similar to an operating wind turbine. This is done by employing the 1D momentum actuator disc theory in PHOENICS, a general purpose Computational Fluid Dynamics (CFD) software.

To test the general applicability of the method, single wind turbine simulations are conducted using 9 different wind turbine models from two manufacturers, 5 Enercon and 4 Siemens wind turbines. The simulations are performed by imposing sheared inflow with hub height wind speeds ranging from 3 m/s up to 25 m/s at hub height. Furthermore, a range of computational parameters are investigated, including the size of the computational domain, the resolution of the domain, the thickness of the actuator disc and the iterative convergence criteria. The main output of the simulations are the wind turbine power production, thrust forces and average wind speed at the disc.

Performing this parametric study has shown that the results are found to be independent of the thickness of the disc. Above a resolution of 8 cells per rotor diameter the power and thrust values were shown not to change noticeably. A convergence criteria of 0.1% was found to be sufficient. Indeed, decreasing the convergence criteria to 0.01% produced a negligible change to the power and thrust results. Whilst resulting in a considerable increase in the time needed to perform the simulations increased considerably.

The results are compared with the experimental power curves provided by the manufacturers for each wind turbine. The output of the actuator disc method was observed to follow the experimental power curves with a difference of 5% for wind speeds in the region of 5m/s to 10m/s. However, as the wind speed increases over this range the difference reached approximately 10% for most cases. The present result shows that actuator disc method is able to provide a reasonable estimation of the conventional wind turbine power output with low computational effort.

News from Shanghai Feiyi

Shanghai Feiyi is presenting PHOENICS at a series of Exhibitions being held in 10 cities in China.

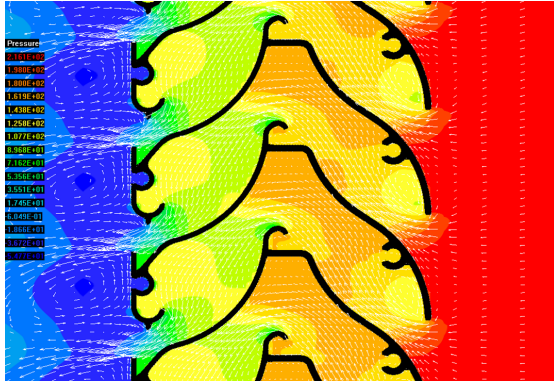
The exhibitions are being arranged by the local Government of Shandong Province to encourage green-building development in the Province.

The photograph below is of the Exhibition in Jinan city which is the capital of Shandong province. The arrow on the right indicates the position of PHOENICS material.



For information on PHOENICS, or to ascertain dates of training courses, please contact <http://www.shanghaifeiyi.cn/>.

News from Coolplug (Germany)



In February/March Coolplug will participate in writing a new VDI standard: "VDI 6020 Blatt 2 „Anforderungen an den Einsatz fluiddynamischer Simulationen in der TGA“ (a requirement for the application of CFD in technical building services). Two PHOENICS Users (Mr Zimmermann and D. Fiedler) will also participate.

The VDI, (German association of Engineers) has some 150,000 members, is very influential and today approximately 200 VDI Standards based on the latest technical developments are produced, annually, by the VDI's technical divisions.

The VDI has systematically built up a set of technical regulations, which contains over 2000 valid VDI Standards extensively covering the broad field of technology. Topics range from securing loads on road vehicles, testing optical fibres up to biomimetics and monitoring consequences of genetically modified organisms. If there is a VDI standard, it is almost mandatory to use it.

Contents

Title	Page
Performance of Personal Ventilation Systems in a Multi-Bed Maternity Ward M Cook, et al, Loughborough University, England	2
Solid Particle Flow in Full-Scale Blast Furnace Reza Safavi Nick, Mefos, Sweden	5
PHOENICS Modelling of Indoor Aerosol Transport and Deposition Bin Zhao et al, Tsinghua University, China	9
Wake Modelling: The Actuator Disc Concept in PHOENICS N Simisroglou et al, WindSim, Sweden	11
News from ACFDA, Canada	5
News from CHAM Japan	10
News from Shanghai Feiyi, China	11
News from Coolplug (Germany), A2TE (Netherlands), ArcoFluid (France), Safe Solutions (Brazil), SSC (Russia).	12

2016 Seminar Dates: CHAM Japan

2016.1.20 Two-phase introduction seminar
 2016.1.18 PHOENICS users seminar for VR-viewer
 2016.1.21 PHOENICS hand-on seminar in Tokyo
 2016.2.11 PHOENICS hand-on seminar in Tokyo
 2016.2.15 PHOENICS hand-on seminar in Osaka
 2016.3.10 PHOENICS hand-on seminar in Tokyo
 2016.2.20 CVD introduction seminar

News from A2TE (the Netherlands)

A Benelux User meeting will be held in the Summer of 2016 in Eindhoven. More information will be provided in future Newsletters.

News from ArcoFluid (France)

PHOENICS in the field of Micro fluidic will be presented at the meeting of CGS μ Lab January 27 & 28 2016 at the center JF of TOTAL in Pau, South West France.

PHOENICS in complex flows will be the subject of several lectures and seminars at the University of Marseille, IRPHE Château-Gombert from mid-April to mid-May 2016.

News from Safe Solutions, (Brazil)

On January 29 2016 Safe Solutions will hold a workshop at Jaragua do Sui to present PHOENICS to some refrigeration companies of the region and also three local Universities.

News from SSC (Russia)

Two PHOENICS- related lecture courses will be held at MPEI in Moscow. More information will be provided in future Newsletters.

Contact Us

Get in touch for more information about our services and products .

Concentration Heat & Momentum Limited (CHAM)

40 High Street
 Wimbledon Village
 London SW19 5AU
 England

Email: phoenics@cham.co.uk

Website: www.cham.co.uk

Telephone: +44 (0) 20 8947
 7651

